AIAA JOURNAL
Vol. 31, No. 3, March 1993

Planar Measurement Technique for Compressible Flows Using Laser-Induced Iodine Fluorescence

Roy J. Hartfield Jr.,* Steven D. Hollo,† and James C. McDaniel‡
University of Virginia, Charlottesville, Virginia 22903

A laser-induced fluorescence technique for conducting planar measurements of temperature, pressure, and velocity in nonreacting, compressible flows has been developed, validated, and demonstrated. Planar fluorescence from iodine, seeded into air, was induced by an argon-ion laser and collected using a liquid-nitrogen cooled charge-coupled device camera. The temperature measurement, which has been described earlier, is used in conjunction with a sophisticated model of the fluorescence excitation spectrum to produce accurate pressure measurements. The demonstration velocity measurements represent the first planar velocity mapping using molecular seed in a highly three-dimensional supersonic flow of practical importance. In the measurement technique, temperature is determined from the fluorescence induced with the laser-operated broadband. Pressure and velocity are determined from the shape and position of the fluorescence excitation spectrum, which is measured with the laser operated narrow band. A parametric relationship has been developed to relate the complex fluorescence excitation spectrum to pressure for specified temperatures. The importance of this novel approach is that it significantly reduces the computational requirements for relating the line shape to pressure, thereby making accurate measurements of pressure at a large number of points in a plane practical. The uncertainty of the measurement is estimated to be 6% for temperature, 5% for pressure, and 25 m/s for velocity.

I. Introduction

LASER-INDUCED iodine fluorescence has been used to conduct quantitative planar measurements of temperature,[1,2] pressure,[3] density,[4,5] velocity,[3,5] and injectant mole fraction[6-9] with varying degrees of accuracy. Also, a unified pointwise laser-induced iodine fluorescence technique for the measurement of temperature,[10] pressure, and velocity has been developed.[11] Previous techniques for planar measurement of thermodynamic parameters using laser-induced iodine fluorescence have been based on simplifying assumptions applied to the fluorescence equation for one or two molecular absorption transitions. The inability of these simplified models to accurately describe the dense iodine absorption spectrum at pressures of current interest (above 1 kPa) has limited the accuracy of previous planar measurements of the thermodynamic parameters in high-pressure air flows. The pointwise measurement technique has provided accurate measurements of pressure and temperature at high pressures by making use of a two-transition temperature measurement technique and a sophisticated model of the iodine fluorescence excitation spectrum.[11]

The two-transition temperature measurement approach requires the use of a tunable dye laser; however, this laser has insufficient power for accurate planar imaging of iodine fluorescence in air flows at moderate pressures (up to 50 kPa). For this reason, the temperature measurement in this work is based on a single-transition technique[1] which is suitable for use with a high-power, argon-ion laser. The pressure is determined from the fluorescence excitation line shape using a model of the fluorescence excitation spectrum and the measured temperature. By employing techniques suitable for use with a high-power laser and by making use of the spectral excitation model in the data reduction, accurate planar measurements of temperature and pressure are obtained in flowfields having a pressure range common to most transonic and low supersonic wind tunnels.

The measurement of velocity using laser-induced fluorescence is based on the velocity-induced Doppler shift in the absorption spectrum. At pressures comparable to those used in this investigation, an additional shift in the absorption spectrum due to collisions, known as the impact shift, contributes significantly to the total frequency shift and must be accounted for in the measurement of velocity. For iodine in air, this impact shift is always to a lower frequency and can be eliminated in a planar, two-component velocity measurement through the use of four counterpropagating beams[12] or three coplanar beams which are not collinear. Alternatively, the impact shift can be calculated from measurements of the local thermodynamic state and subtracted from the total shift.[11] For flowfield planes in which optical access is available from only one side of the flowfield facility, the use of counterpropagating beams is impossible and the use of three noncollinear beams to eliminate the impact shift leads to inaccurate results because of limitations on allowable laser sheet directions. In that case, accurate planar measurements of the velocity field are possible only if accurate measurements of the temperature and pressure can be conducted. In this work, the wind-tunnel geometry precluded the elimination of the impact shift; hence, the impact shift was calculated using the measurements of pressure and temperature at each point in the flowfield.

The overall measurement approach reported herein includes the initial temperature measurement, the determination of pressure from a measured line shape and temperature, and the determination of Doppler shifts for two velocity components from measured total shifts in the absorption spectrum, with the impact shift calculated from the measured pressure and temperature. A description of the analytical development of this approach, some technique validation experiments, and some sample results in a complex compressible flowfield are included.

Presented as Paper 92-0141 at the AIAA 30th Aerospace Sciences Meeting, Reno, NV, Jan. 6-9, 1992; received Jan. 14, 1992; revision received Aug. 17, 1992; accepted for publication Aug. 21, 1992.

*Research Assistant, Department of Mechanical and Aerospace Engineering; currently Assistant Professor of Aerospace Engineering, Auburn University, Auburn, AL 36849-5338. Member AIAA.

†Research Assistant, Department of Mechanical and Aerospace Engineering. Member AIAA.

‡Associate Professor, Department of Mechanical and Aerospace Engineering. Member AIAA.

II. Laser-Induced Iodine Fluorescence: Planar Measurement Technique

A. Temperature Measurement

When excitation is provided by a laser with a gain profile that is considerably broader than the absorption transition line width, the resulting fluorescence signal at high pressures is primarily a function of temperature. The fluorescence signal that results from the excitation of iodine by the approximately 6-GHz gain profile of the 514.5-nm line of the argon-ion laser contains contributions from many absorption transitions; however, it has been shown[1] that a simplified model of the fluorescence based on the signal obtained in the limit of high pressure (approximately 20 kPa) from only two prominent absorption transitions in the vicinity of 514.5 nm accurately describes the fluorescence as a function of the temperature over a wide range of flowfield conditions. In addition, this fluorescence is a monotonic function of temperature over the temperature range of interest; hence, it can be used to measure temperature. This technique for obtaining temperature is used herein and is described in detail in Ref. 1.

B. Pressure Measurement and Fluorescence Excitation Model

Collisional broadening of molecular absorption transitions is a function of both pressure and temperature. If the temperature is known, the pressure can be determined from measurements of collisional broadening. For isolated absorption transitions, collisional broadening can be determined from the width of the absorption transition; however, because of the high density of the iodine absorption spectrum, contributions from adjacent transitions can dramatically alter the profile of an absorption transition, making it necessary to use a model of the fluorescence excitation spectrum to relate a measured line shape to collisional broadening or, more directly, pressure. A detailed model of the iodine fluorescence excitation spectrum in the vicinity of 514.5 nm has been developed for this purpose.

Because of the fundamental importance of the spectral model to the measurement technique, a brief description of the approach used in the development of the model is given. For narrow band excitation, the fluorescence signal is given by[13]

$$S_f = CB_{12}I(X)\frac{A_{21}}{A_{21}+Q}\left\{\frac{V(D,B)}{\Delta\nu_D}\right\}F_1(T)N_{I_2} \tag{1}$$

In Eq. (1), S_f is the fluorescence intensity, C a constant that includes detector quantum efficiency and optical collection efficiency, B_{12} the Einstein coefficient for absorption, $I(X)$ the laser intensity at the measured point X, A_{21} is the fluorescence decay rate of the molecule (the Einstein coefficient for emission), Q the collisional quenching rate, $F_1(T)$ the Boltzmann population fraction of the energy level being excited in the ground state, and N_{I_2} the number density of the molecular species being irradiated—iodine in this case. The quantity $A_{21}/(A_{21}+Q)$ is referred to as the Stern-Volmer factor and is the ratio of the fluorescence decay rate to the total decay rate of the excited state.

The term in braces in Eq. (1) describes the absorption line shape. The numerator in this term is the Voigt function, which contains effects of both collisional Doppler broadening. The parameters for the Voigt profile are the detuning D and the broadening B. The denominator in the term in braces, $\Delta\nu_D$, is the Doppler line width. The Voigt function is the convolution of Gaussian (thermal) and Lorentzian (collisional) line broadening and is represented as[14]

$$V(D,B) = \frac{B}{\pi}\int_{-\infty}^{+\infty}\frac{e^{-y^2}dy}{B^2+(D-y)^2} \tag{2}$$

The broadening parameter B, is given by[13]

$$B = \sqrt{\ell n\, 2}\,\frac{\Delta\nu_c}{\Delta\nu_D} \tag{3}$$

where $\Delta\nu_c$ is the collisional line width. The collisional line width for iodine has been investigated extensively and can be represented by[15]

$$\Delta\nu_c = C_b(P/T^{0.7}) \tag{4}$$

where C_b is the effective broadening cross section. The Doppler line width is a function of temperature and is given by

$$\Delta\nu_D = \sqrt{\frac{8\,\ell n(2)kT}{mc^2}}\,\nu_0 \tag{5}$$

where m is the mass of a molecule, k the Boltzmann constant, c the speed of light, and ν_0 the molecular center frequency with no Doppler shift. The 514.5-nm line of the argon-ion laser coincides with the strong, blended, P13-R15 absorption transition in iodine. Because of the high power of this laser line and the strong iodine absorption coincidence, this is the excitation wavelength selected. The iodine Doppler line width at 514.5 nm is 442 MHz at 298 K; however, the total iodine line width at pressures well below 0.1 kPa is approximately 1.2 GHz. This added line width is caused by the hyperfine structure of the rotational transitions.[16] For the purpose of evaluating Eq. (1), this hyperfine width is taken to be 800 MHz (the difference between the Doppler line width at 298 K and the measured line width at very low pressure) and is added to the Doppler line width. (It should be noted that, at pressures exceeding 10 kPa, collisional broadening from both the transition under consideration and adjacent transitions dominate the absorption line shape and the calculation of the iodine fluorescence excitation spectrum is relatively insensitive to the value of the hyperfine width.) The detuning parameter D is given by[14]

$$D = 2\sqrt{\ell n(2)}\,\frac{\Delta\nu}{\Delta\nu_c} \tag{6}$$

where $\Delta\nu$ is the detuning from the absorption line center.

For a homogeneously seeded fluid that behaves as an ideal gas,

$$N_{I_2} = f_s N_T = f_s(P/kT) \tag{7}$$

where N_T is the total number density, f_s the seeding fraction, and P the thermodynamic pressure. The collisional quenching rate scales with collisional frequency, so

$$Q = C_q\left(P/\sqrt{T}\right) \tag{8}$$

where C_q is the effective quenching cross section.

If the assumptions are made that the ground electronic state remains in Boltzmann equilibrium during excitation, the molecule vibrates as a harmonic oscillator, and the temperatures of interest are much greater than the characteristic rotational temperature (0.0538 K for iodine), the population fraction is given by

$$F_1 = GHF(J)\left\{\left[2(2J+1)(\Theta_r/T)\right]e^{-J(J+1)(\Theta_r/T)}\right\} \times\left\{e^{-\nu(\Theta_v/T)}\left[1-e^{-(\Theta_v/T)}\right]\right\} \tag{9}$$

In this equation, $GHF(J)$ is the hyperfine degeneracy of the rotational state,[16] J the rotational quantum number, ν the vibrational quantum number, Θ_r the characteristic rotational temperature, and Θ_v the characteristic vibrational temperature (308.62 K for iodine).

Using the relationships in Eqs. (2–9) and experimentally determined constants, Eq. (1) can be used to calculate the fluorescence signal as a function of excitation wavelength, pressure, and temperature. (The determination of the constants employed in this model is described in detail in Ref. 17.) At very low thermodynamic pressures, the dense iodine ab-

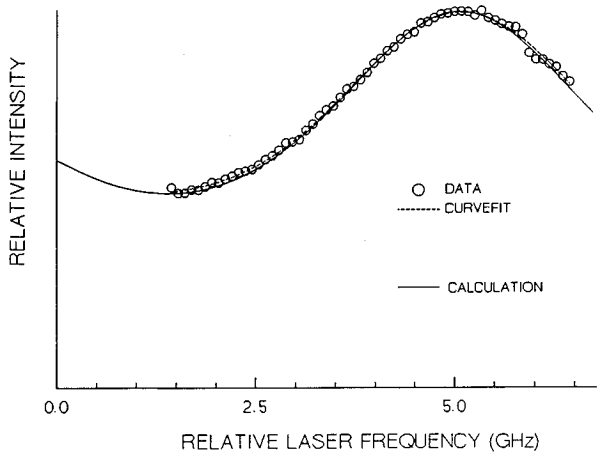

Fig. 1 Comparison of calculated and measured fluorescence excitation spectra.

sorption spectrum is a series of discrete, distinguishable lines and blended, or spectrally coincident, lines; however, for modest pressures, the absorption in the spectral vicinity of a single transition is affected by the line broadening of relatively distant neighboring transitions. For that reason, the fluorescence signal at a specified spectral location is calculated by summing the fluorescence signals, calculated using Eq. (1), from 38 absorption transitions in the vicinity of 514.5 nm. These transitions span a 64-GHz spectral region centered on the line center of the 514.5-nm line of the argon-ion laser and include all lines which contribute at least 1% of their line center value to the total fluorescence signal at nominal conditions of 100 kPa and 300 K.

To develop confidence in the ability of the model to correctly calculate the fluorescence excitation spectrum, comparisons between calculated and measured absorption line profiles at known thermodynamic conditions were conducted. To demonstrate the ability of the model to accurately predict the line shape, a sample comparison of calculated and measured spectra is given in Fig. 1. The thermodynamic conditions for this comparison are 167 K and 34.8 kPa, the freestream conditions for the Mach 2 flow demonstration flow. The data in Fig. 1 were collected by tuning the single axial mode argon-ion laser across the central 5-GHz portion of its gain profile and collecting the fluorescence broadband. From this figure it can be seen that the calculation is in excellent agreement with both the data and a parametric curve fit to the data. Comparisons of measured and calculated fluorescence excitation spectra at other known thermodynamic conditions showed similar agreement.[17]

To accurately determine the absorption line shape and line center, a parametric curve, as shown in Fig. 1, is fit to the spectral data. The functional form that was found to best fit the data was a Gaussian plus a constant. It is very important to note that this parametric function describes a complex line shape composed of the Voigt line shape for the primary transition and overlapping wings of the Voigt profiles of adjacent transitions. These absorption lines are dominated by collisional broadening and the parametric representation of the overall line shape by a Gaussian function should not be confused with Doppler broadening. Another critical point is that the constant in this parametric function arises primarily from the broadening of adjacent transitions and not from substantial background scattered light or fluorescence. Background images collected with the laser sheet in the wind tunnel but with no iodine seeding typically contained less than 1% of the measured line center fluorescence signals and this background was subtracted from the data before the analysis began. In addition to subtracting this background due to scattering, extensive examinations of measured fluorescence excitation spectra have led the authors to conclude that there is no significant background introduced by the seeding process. Further discussion of this matter is given subsequently.

The shape of the fluorescence excitation spectrum is strongly dependent on the pressure and temperature. With a previously measured temperature and a measured fluorescence excitation spectrum at each point in the planar image, pressure could be obtained by incrementing its value in the model until a best fit to the measured spectra is obtained; however, this would be very computationally expensive for planar measurements. To obtain pressure from the measured excitation spectra with improved computational efficiency, a relationship between some parameter describing the spectral shape and the pressure must be established. The parameter chosen to relate the spectral shape to the pressure is the ratio of the fluorescence signal at 1.7 GHz (20 argon laser longitudinal mode spacings) away from the absorption line center to the fluorescence signal at the spectral center. Using the fluorescence model, it was estimated that at 1.7 GHz the sensitivity of this signal ratio to pressure is maximized for the pressure range of current interest.

A plot of the calculated ratio of the 1.7-GHz off-center signal to the centerline signal as a function of pressure for 100, 200, and 300 K is shown in Fig. 2. Even at relatively low pressures (10 kPa), this signal ratio is an extremely complicated function owing to the density of the iodine absorption spectrum. To relate this signal ratio to the thermodynamic parameters, the following scheme was employed. The signal ratio was calculated using the fluorescence model over the anticipated pressure measurement range for 11 temperatures in the anticipated measurement range. A fifth-order polynomial in pressure was then fit to the calculated ratio for each of the selected temperatures. Next, a fourth-order polynomial in temperature was fit to each of the six coefficients in the fifth-order polynomial in pressure. The result is a fifth-order polynomial in pressure, with temperature-dependent coefficients, which describes the signal ratio for all expected temperatures and pressures and has the following form:

$$\text{ratio} = A(T) + B(T)P + C(T)P^2 + D(T)P^3 + E(T)P^4 + F(T)P^5 \tag{10}$$

It should be noted that the Gaussian curve fit to the data is, by definition, symmetric; however, the actual fluorescence spectrum (experimental and calculated) can be slightly asymmetric. Since there is no justification for granting preference to either side of the absorption transition, the calculated ratio was obtained using the average of the calculated signal at 1.7 GHz to the right and left of the spectral center. To obtain pressure from the measured signal ratio (obtained from the parametric Gaussian plus constant curve fit to the data), the value of each of the coefficients in this polynomial was calculated from the previously measured temperature. The polynomial was then solved numerically for the pressure.

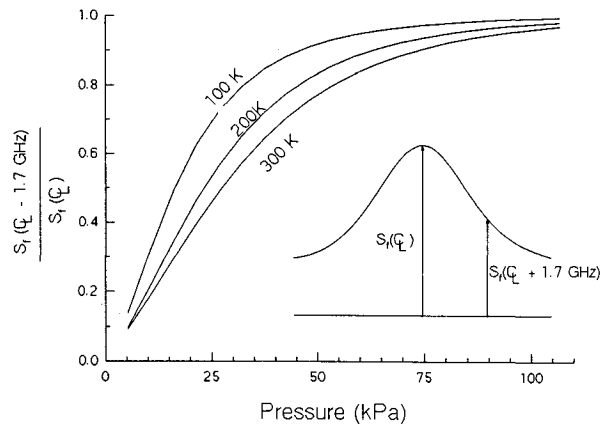

Fig. 2 Parameter used to obtain pressure measurement.

From the plot shown in Fig. 2, it is apparent that the sensitivity of the pressure measurement is high at low pressure and low at high pressure. This is expected from a pressure measurement technique that relies on collisional broadening of a molecular absorption transition because, at low pressure, transitions are narrow and their shapes are dramatically affected by changes in pressure. At high pressure, the lines in the molecular absorption spectrum are broadened and blended together to form a nearly flat absorption spectrum which cannot be substantially affected by small changes in pressure. By employing the measurement scheme for pressure just described, the sophistication of the spectral model is preserved in the data reduction without requiring a full spectral model curve fit at each data point.

C. Velocity Measurement

The Doppler shift in the molecular absorption spectrum has been previously employed to conduct velocity measurements.[3,5,11,18,19] The Doppler shift is related to the velocity component in the direction of laser beam propagation by[5]

$$\Delta\omega_D = \boldsymbol{k} \cdot \boldsymbol{u} \tag{11}$$

where $\Delta\omega_D$ is the Doppler shift given in rad/s, $\boldsymbol{k}$ is the wave vector of magnitude $2\pi/\lambda$ in the direction of the laser beam propagation, and $\boldsymbol{u}$ is the velocity vector describing the convective motion of the irradiated molecules. The collisional impact shift discussed earlier contributes significantly to the total shift of the molecular absorption transition at moderate thermodynamic pressures; hence, the total shift cannot be used directly to obtain measurements of velocity components. The thermodynamic dependence of the impact shift has been extensively investigated and is given by[15]

$$\Delta\nu_I = -C_I(P/T^{0.7}) \tag{12}$$

where C_I is the impact shift constant. Because of the limited optical access, the impact shift was calculated from measured pressures and temperatures using Eq. (12) and an experimentally determined impact shift constant.[17] The impact shift was then subtracted from the total shift to determine the Doppler shift in the direction of laser sheet propagation. These Doppler shifts were then used to calculate the respective velocity components using Eq. (11). The angles for the laser sheet directions were + 45 and − 45 deg to the freestream direction so that the angle between the two laser sheet directions was 90 deg. This arrangement was chosen so that the sensitivity of the velocity measurement would be the same in all directions.

III. Flowfields and Experimental Setup

For measurement techniques to be used with confidence in complex, unknown flows, the techniques must first be verified in flows with known variations in the measured parameters. The flowfield selected for the verification of the measurement approach described previously is Mach 2 flow over a rearward-facing step. The thermodynamic parameters in the resulting two-dimensional expansion fan can be accurately calculated. A schematic of this flowfield is shown in Fig. 3. The Mach 2 inlet flow expands toward the wall downstream of the step through the centered Prandtl-Meyer expansion fan. A shear layer separates the higher Mach number flow downstream of the expansion from the recirculation zone in the base of the step. The flow is turned back parallel to the test section wall and compressed through an oblique shock wave. The angle between the shear layer and the wall of the test section was measured to be 15.5 deg using a shadowgraph. This angle corresponds to the flow turning angle for the expansion fan and from this angle the conditions downstream of the expansion fan can be calculated. After verifying the measurement techniques in this flowfield, measurements were conducted with sonic air injection at the centerline along the top wall at both three step heights and seven step heights downstream of the step. For this flowfield, the step height is 3.18 mm and the diameter of the injectors is 1.98 mm. This flow with injection is highly three dimensional and has been chosen as a validation flowfield for compressible computational fluid dynamic codes.[20] Some sample measurement results in this flowfield will be presented.

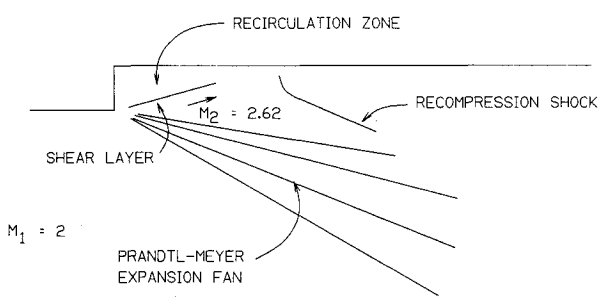

Fig. 3 Flowfield schematic for Mach 2 flow over a step.

The flowfield facility consists of a dry air source, an iodine mixing vessel, a Mach 2 wind tunnel, and an activated charcoal filter for removing the iodine before the air is exhausted into the atmosphere. The tunnel is constructed of teflon-coated aluminum for corrosion resistance and is equipped with fused silica windows on three sides of the test section for excellent optical access.

The primary components of the optical system are a large-frame argon-ion laser (Spectra Physics Model 171) and a liquid-nitrogen-cooled charge-coupled device (CCD) camera (Photometrics CH210). For the narrow-band measurements the output frequency of the large-frame argon-ion laser with a 3-MHz line width is tuned using an intercavity etalon. A power meter is used to record the laser power at each spectral location and a scanning interferometer is used to set the relative laser frequency. The absolute laser frequency is monitored by collecting, with a photomultiplier tube, the fluorescence excitation spectrum in a low-pressure iodine static cell as the laser is tuned across the gain profile. Additionally, the beam from a small-frame argon-ion laser is passed into the test section immediately upstream of the laser sheet. The fluorescence induced by this beam is recorded on the edge of the CCD array to record the iodine seeding fraction variation during the experiment. The output of the laser power meter and the photomultiplier tube are recorded using a data acquisition system connected to a microcomputer.

The laser beam is converted to a thin sheet using a 6.4-mm focal length cylindrical lens and a spherical lens with a focal length which depends on the desired width of the sheet. For this work, the sheet thickness was less than 200 μ and the sheet width was less than 10 cm. For the broadband measurements, the final turning mirror, which directs the sheet into the wind tunnel, and the camera were mounted on a single computer-controlled translation stage which has 1-μ resolution. This arrangement insured that the field of view and focus of the camera remained constant for the various flowfield planes in which measurements are conducted. For the narrow-band measurements, two translation stages were used for laser sheet positioning.

IV. Experimental Results

A. Measurement Verification Experiments

To completely represent the spatially extensive data obtained using planar measurement techniques, contour plots of pressure and temperature and vector plots of the velocity field are needed. Some of these plots are included. For a more detailed quantitative illustration of the capability of the planar measurement techniques, line profiles showing comparisons of measured and calculated values in the Mach 2 flow over a step

verification flowfield are also included. The average stagnation conditions for the verification measurements were 301 K and 273 kPa. With these stagnation conditions and the Mach 2 nozzle, the freestream conditions were 167 K, 34.8 kPa, and 520 m/s. It should be noted that this paper focuses on the planar measurement technique. An extensive discussion of the flowfield data and its use in computer code validation is presented in Ref. 21.

1. Temperature

A contour plot of the measured two-dimensional temperature distribution for Mach 2 flow over a rearward-facing step is presented in Fig. 4. The isotherms in the expansion fan are essentially straight lines along the expansion waves. Some small perturbations in these waves caused by weak characteristic waves from the facility nozzle are detectable. A group of isotherms coalesce along the shear layer because of the large-temperature gradient across this shear layer. From this plot, it can be seen that the high-temperature recirculation zone stretches out into a relatively thick layer along the top wall. A temperature rise across the oblique shock is also noted. In the vicinity of the step, significant curvature of the isotherms is evident. Also, the higher-temperature isotherms along both walls of the nozzle exhibit the presence of the boundary layer.

Figure 5 is a plot showing the one-dimensional temperature profile normal to the top wall at a location 10 mm downstream of the rearward-facing step. For this and subsequent plots, $z = 0$ corresponds to the top wall of the tunnel downstream of the step and the bottom wall of the tunnel is located at $z = 20.12$ mm. The dotted line represents the measurement, the dashed line represents a two-dimensional analytical calculation assuming an isentropic expansion, and the solid line represents a Navier-Stokes numerical calculation performed at the NASA

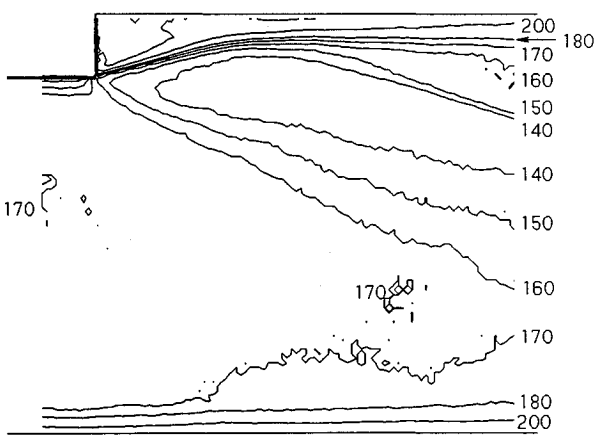

Fig. 4 Mach 2 flow over a rearward facing step: temperature distribution, K.

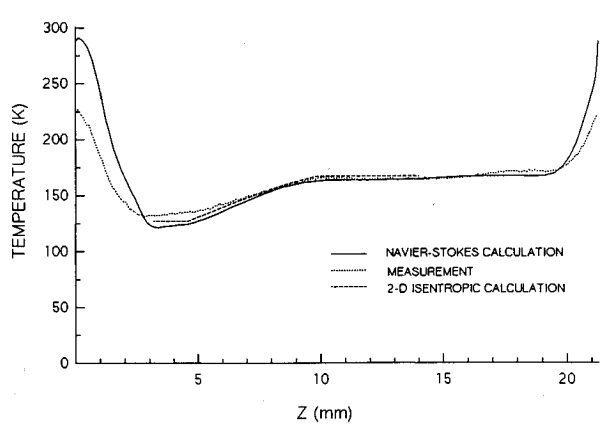

Fig. 5 Comparison of temperature profiles at 10 mm downstream of step.

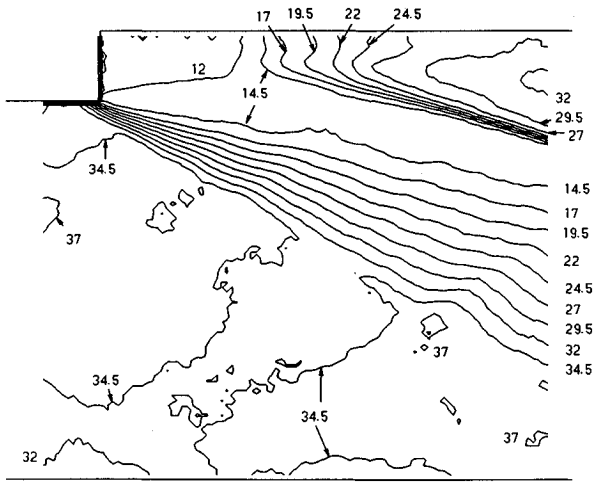

Fig. 6 Mach 2 flow over a rearward facing step pressure distribution, kPa.

Langley Research Center.[22] The region of this profile that is most useful for measurement technique verification is the isentropic region between approximately $z = 3$ mm and $z = 17$ mm. The separated flow behind the rearward-facing step and the temperature recovery in the boundary layers are not as well calculated as the isentropic region. The disagreement between the calculation and the measurement in the nonisentropic regions is currently unresolved. In the verification portion of the flowfield at this location, the maximum disagreement between the measurement and the analytical calculation is 5 K and the maximum difference between the measurement and the Navier-Stokes calculation is 7 K. Both of these differences are within the estimated 6% uncertainty of the temperature measurement technique presented in Sec. V.

2. Pressure

The pressure measurement technique was verified for pressures ranging from 13 to 35 kPa in the rearward-facing step flowfield. A contour plot of the measured pressure distribution for this flowfield is shown in Fig. 6. The pressure contours in the expansion fan lie along the expansion waves and, except for the influence of the characteristic wave from the nozzle, are seen to be straight lines. The pressure in the base of the step is quite uniform and is only slightly less than the pressure in the flow area immediately downstream of the expansion fan. The reattachment region and shock formation are apparent near the top wall. At the beginning of the shock formation, the contours are well separated but farther downstream they coalesce into a well-defined oblique shock. It is very important to note that, while strong gradients in the temperature field occur across the boundary layers, the pressure is observed to be relatively uniform across the boundary layers as expected. The 34.5-kPa contours indicate the presence of a characteristic wave in the nozzle, as mentioned earlier. Noteworthy is the fact that the curvature observed in the temperature contours near the step is not present in the pressure contours because the pressure is approximately constant through a boundary layer. The pressure contours emanate from the origin of the expansion fan, which is approximately 1.5 mm upstream of the step due to the suction applied to the boundary layer by the lower pressure in the base of the step. Additionally, there is only a small pressure gradient across the shear layer, as expected.

To quantitatively verify the accuracy of the pressure measurement, a comparison is made between the measured pressure distribution, the two-dimensional isentropic calculation of the pressure field across the Prandtl-Meyer fan, and the Navier-Stokes calculation referenced earlier. The comparisons are made at the same location 10 mm downstream of the step and are shown in Fig. 7. In the isentropic region of this profile used for measurement verification, the maximum disagree-

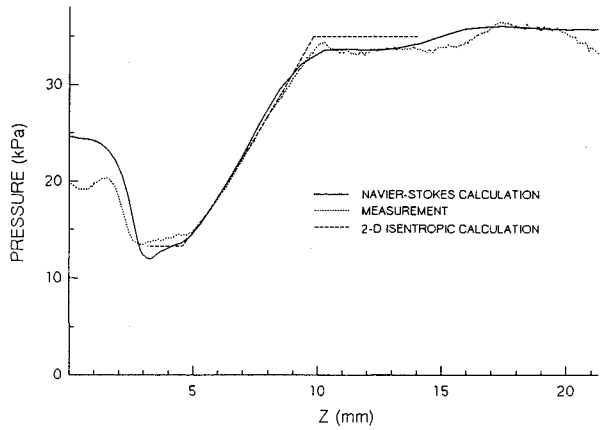

Fig. 7 Mach 2 flow over a step: comparison of measured pressure profile to Navier-Stokes calculation at 10 mm downstream of step.

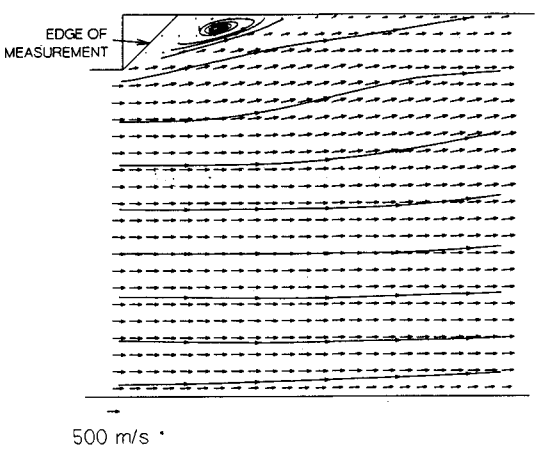

Fig. 8 Mach 2 flow over a step: velocity distribution.

ment between the Navier-Stokes calculation and the measurement is 1.5 kPa at the exit of the expansion fan. This disagreement is well within the 5% uncertainty in the pressure measurement presented in Sec. V.

3. Velocity

A full view of the measured velocity field showing the streamlines in this two-dimensional flowfield is given in Fig. 8. A detailed vector plot of the velocity field near the base of the step is shown in Fig. 9. For clarity, the grid for the plotted velocity data points shown in Fig. 9 contains only 1/16 of the total measurement points and the plot shown in Fig. 8 only 1/144 the total points. For both of these figures, a 500-m/s vector is included to indicate the scale of the vector magnitudes. In Fig. 8, streamlines drawn using TECPLOT®, a computer plotting package, indicate the turning of the freestream by the expansion fan and oblique shock wave. As expected, a well-defined recirculation zone in the base of the step can be seen in the streamlines in Fig. 8 and in the velocity vectors in Fig. 9. The detail of the recirculation is quite apparent and underscores the capability of this technique to accurately resolve velocity components which are less than 10% of the 520-m/s freestream. No vectors are plotted in the corner of the step because the step casts a shadow in this area for one of the laser sheet directions.

Profiles of the U (horizontal) and V (vertical) velocity components at the same location 10 mm downstream of the step are used to quantitatively verify the measurement technique. This plot is shown in Fig. 10. As before, the dashed line showing the two-dimensional isentropic calculation is plotted in the portion of the flowfield used for verification. In the freestream, the measured V component of velocity is 0, in agreement with both calculations and the one-dimensional exit flow. The magnitude of the V component is systematically high in the leading portion of the expansion fan by as much as 25 m/s and is systematically low by as much as 25 m/s at the fan exit. There is excellent agreement in the expansion fan for the U component; however, at the nozzle exit, the measured U component is systematically low by approximately 25 m/s. From these comparisons and a detailed error analysis, it appears that the maximum error in the velocity measurement technique under these conditions is 25 m/s, or 5% of the freestream value.

B. Supersonic Combustor Results

This measurement technique was developed as part of an extensive experimental program designed for the purpose of validating computational fluid dynamic codes used in the design of SCRAMJET engines. As a part of that validation effort, this technique has been used to produce comprehensive maps of the temperature, pressure, and velocity distributions in a generic SCRAMJET combustor geometry which offers significant computational challenges. This flowfield geometry, described earlier, is staged transverse injection behind a rearward-facing step into a Mach 2 freestream. For the combustor results presented herein, the average stagnation conditions were 301 K and 277 kPa and the freestream conditions were 167 K, 35.4 kPa, and 520 m/s. A complete presentation of the extensive data set for this flowfield can be found in Reference 21.

To demonstrate the ability of this planar technique to conduct accurate, comprehensive surveys of flowfield parameters in unknown and highly three-dimensional compressible flows, contour plots of temperature and pressure measurements conducted in the centerline plane of the staged transverse injector flowfield are included in Figs. 11 and 12. A vector plot of the velocity distribution on the tunnel centerline in the near field of the first injector in this flowfield is shown in Fig. 13. In the contour plots, the step and the location of the injectors are indicated. With injection, the expansion fan is not nearly as

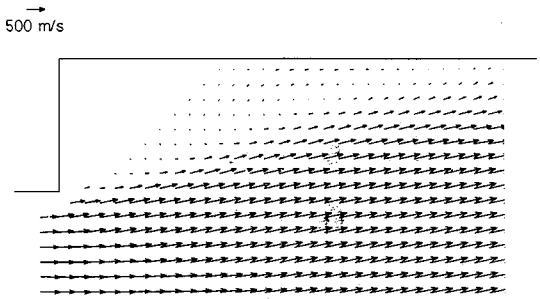

Fig. 9 Mach 2 flow over a step: velocity distribution in vicinity of step.

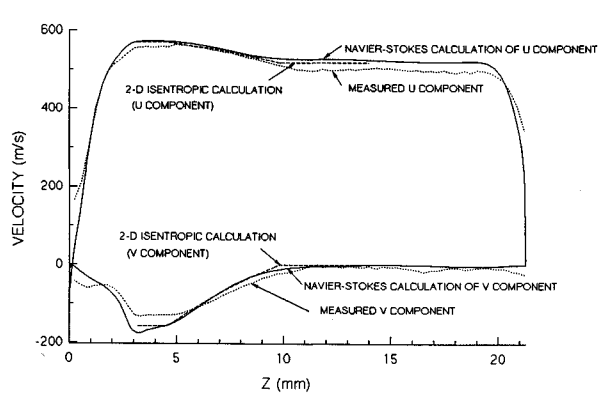

Fig. 10 Mach 2 flow over a step: comparison of measured velocity components to Navier-Stokes calculation at 10 mm downstream of step.

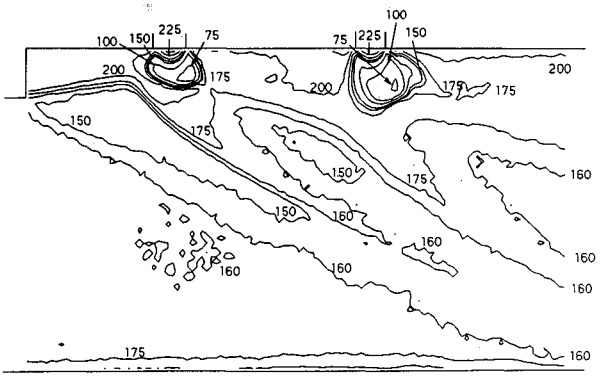

Fig. 11 Staged transverse injection: temperature distribution, K, at centerline.

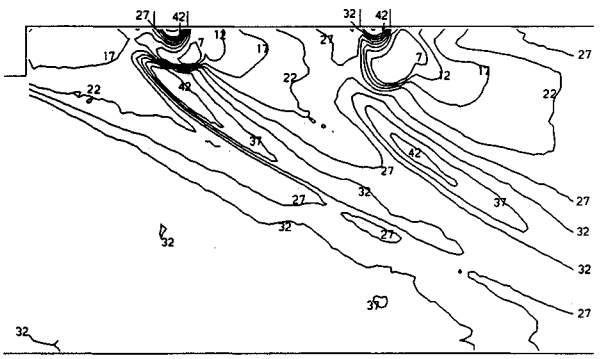

Fig. 12 Staged transverse injection: pressure distribution, kPa, at centerline.

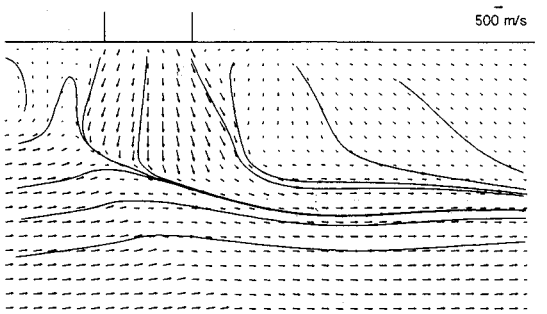

Fig. 13 Staged transverse injection behind a rearward facing step: velocity distribution near first injector.

extensive as without injection due to the pressure rise in the base of the step with injection. A strong temperature gradient is reflected in the coalescence of the isotherms in the shear layer between the high-velocity flow downstream of the expansion and the low-velocity flow in the recirculation zone; however, the pressure gradient in this region is quite low, as expected. The injectors are both highly underexpanded, producing the low pressure and temperature injector cores. Only a very small area of the flow is represented in the velocity vector plot shown in Fig. 13 in order that flow details, such as the high shear area immediately in front of the injector and the velocity distribution in the core of the jet, could be emphasized. Measurements of injectant mole fraction in crossflow planes of this flowfield have indicated that the flowfield is very nearly symmetric about the centerline; therefore, the third velocity component in this plane is negligible. For this reason, streamlines can be plotted along with the velocity vectors and are included in Fig. 13.

V. Factors Contributing to Experimental Uncertainty

A fundamental concern relevant to the use of iodine vapor in the quantitative measurement of flowfield parameters in supersonic flows is vapor condensation. Iodine is mixed with air by passing the air over crystals in a mixing vessel. The air is not saturated with iodine vapor in the mixing vessel; however, as the static temperature decreases in the supersonic flow, saturation and supersaturation are expected to occur; therefore, the possibility of condensation must be addressed and investigated. After running the Mach 2 facility used for this investigation for periods of time exceeding one-half hour, varying amounts of iodine condensation can be observed on the walls of the wind tunnel in the form of a thin iodine film. The thickness of this film varies. It is barely observable in some areas and is seen to increase in regions immediately downstream of shocks; however, the amount of iodine collected on the tunnel walls is a minute fraction of the iodine passed through the tunnel. An additional indication of the existence of significant iodine condensation would be increased background signals at off-resonant positions in the emission spectra collected in regions of the flow where condensation is most likely to occur. Data downstream of strong shocks and in recirculation zones were examined in detail and the off-resonant signals were found to be approximately equal to, or less than, the signals predicted from calculations of the fluorescence excitation spectra. This is not conclusive proof that no significant condensation exists and condensation remains a potential source of systematic error; however, based on the analysis of data points herein, no direct evidence of significant condensation was observed.

Noteworthy is the fact that an assumption of high pressure has been made in the development of the model for the temperature measurement and some of the measurements using this technique are reported for pressures below the stated high-pressure limit (20 kPa). This has been done in part because good agreement between measured and predicted temperatures is observed in isentropic expansions to pressures well below the high-pressure limit stated in the development of the technique. Estimated systematic uncertainties resulting from the use of the temperature measurement technique at low pressures have been included in a detailed error analysis.[17]

The measurement technique as developed herein is inherently time averaged. The images collected for the temperature measurement and each image used to generate the spectral data for pressure and velocity measurement were averaged by approximately 1-min exposures on the collection array camera. An implicit assumption is that, since this exposure time is long compared to characteristic flow times, the data collected will produce the time average of the measured quantity. A computer-controlled, micron-resolution translation stage was used to insure accurate spatial overlap between the broadband data and the spectrally-resolved data. Additionally, both the broadband data and the spectrally resolved data were collected on the same day and stagnation conditions were maintained to within 0.5% throughout the two data sets.

A detailed uncertainty analysis is given in Ref. 17. The analysis approach and results are briefly presented here. For estimates of the uncertainty in the pressure and temperature, analytical techniques based on logarithmic differentiation were used to estimate random errors resulting directly from instrument-related signal measurement uncertainties and photon statistical noise. Added into these calculations were estimates of systematic errors introduced by approximations in the fluorescence model used in the data reduction. The resulting uncertainties were also compared to differences between the measured quantities and known flowfield values. The uncertainties in the velocity measurement were estimated based on the width of the absorption transition and estimates of the uncertainty in the calculated impact shift owing to the uncertainties in the measurement of temperature and pressure. The measurement uncertainties for each of the parameters are functions of the thermodynamic conditions. Nominal values for the measurement uncertainties at 35 kPa and 200 K are 6% for temperature, 5% for pressure and 25 m/s for velocity.[17]

It should be noted that the temperature measurement is the

most susceptible to systematic error because it relies on a single absolute signal level measurement. An improved two-transition approach for determining temperature using an argon-ion laser with an increased tuning range is currently under development at the University of Virginia.

VI. Concluding Remarks

A technique for conducting accurate planar measurements of the thermodynamic parameters and velocity in nonreacting, compressible, and highly three-dimensional flows has been developed. This technique has been validated in the known flowfield of Mach 2 flow over a rearward-facing step. Finally, the technique has been used to produce an extensive set of measurements of temperature, pressure, and velocity distributions in a generic SCRAMJET combustor design.

The approach presented herein represents a significant step in the advancement of planar techniques for the measurement of thermodynamic parameters and velocity in compressible air flows with a pressure range common to many transonic and low-supersonic wind tunnels. As developed herein, the measurement technique is directly applicable only to low enthalpy dry air flows. With some slight modifications to the fluorescence excitation model, this technique could be adapted for dry nitrogen flows. The technique offers the capability of providing significant insights into complex compressible flow phenomena and of providing accurate, spatially-complete data suitable for comparisons with computational fluid dynamic calculations.

Acknowledgment

This work has been supported by the NASA Langley Research Center under Grant NAG-1-795, G. Burton Northam, technical monitor.

References

[1]Hartfield, R. J., Jr., Hollo, S. D., and McDaniel, J. C., "Planar Temperature Measurement in Compressible Flows Using Laser-Induced Iodine Fluorescence," *Optics Letters,* Vol. 16, No. 2, 1991, pp. 106–108.

[2]Ni-Imi, T., Fujimoto, T., and Shimizu, N., "Method for Planar Measurement of Temperature in Compressible Flow Using Two-Line Laser-Induced Iodine Fluorescence," *Optics Letters,* Vol. 15, No. 16, 1990, pp. 918–920.

[3]Hiller, B. H., and Hanson, R. K., "Simultaneous Planar Measurements of Velocity and Pressure Fields in Gas Flows Using Laser-Induced Fluorescence," *Applied Optics,* Vol. 27, No. 1, 1988, pp. 33–48.

[4]McDaniel, J. C., Baganoff, D., and Byer, R. L., "Density Measurement in Compressible Flows Using Off-Resonant Laser-Induced Fluorescence," *Physics of Fluids,* Vol. 25, No. 7, 1982, pp. 1105–1107.

[5]McDaniel, J. C., "Quantitative Measurement of Density and Velocity in Compressible Flows Using Laser-Induced Iodine Fluorescence," AIAA 21st Aerospace Sciences Meeting, AIAA Paper 83-0049, Reno, NV, Jan. 1983.

[6]Hartfield, R. J., Jr., Abbitt, J. D., III, and McDaniel, J. C., "Injectant Mole Fraction Imaging in Compressible Mixing Flows using Planar Laser-Induced Iodine Fluorescence," *Optics Letters,* Vol. 14, No. 16, Aug. 1989, pp. 850–852.

[7]Abbitt, J. D., Hartfield, R. J., Jr., and McDaniel, J. C., "Mole Fraction Imaging of Transverse Injection in a Ducted Supersonic Flow," *AIAA Journal,* Vol. 29, No. 3, 1991, pp. 431–435.

[8]Hollo, S. D., Hartfield, R. J., Jr., and McDaniel, J. C., "Injectant Mole Fraction Measurements of Transverse Injection in Constant Area Ducts," AIAA 21st Plasmadynamics and Lasers Conference, AIAA Paper 90-1632, Seattle, WA, June 1990.

[9]Hartfield, R. J., Jr., Hollo, S. D., and McDaniel, J. C., "Experimental Investigation of a Supersonic Swept Ramp Injector Using Laser-Induced Iodine Fluorescence," AIAA 21st Fluid Dynamics, Plasma Dynamics and Lasers Conference, AIAA Paper 90-1518, Seattle, WA, June 1990.

[10]Fletcher, D. G., and McDaniel, J. C., "Temperature Measurement in a Compressible Flow Field Using Laser-Induced Iodine Fluorescence," *Optics Letters,* Vol. 12, No. 1, 1987, pp. 16–18.

[11]Fletcher, D. G., and McDaniel, J. C., "Laser-Induced Iodine Fluorescence Technique for Quantitative Measurement in a Nonreacting Supersonic Combustor," *AIAA Journal,* Vol. 27, No. 5, 1989, pp. 575–580.

[12]McDaniel, J. C., "Laser Methods for Nonintrusive Measurement of Supersonic Hydrogen-Air Combustion Flowfields," *Annual Proceedings,* Laser Inst. of America, Toledo, OH, Vol. 67, 1988, pp. 209–218.

[13]McDaniel, J. C., "Nonintrusive Pressure Measurements with Laser-Induced Iodine Fluorescence," Combustion Diagnostics by Nonintrusive Methods, Vol. 92, Progress in Astronautics and Aeronautics, AIAA, New York, 1984, pp. 107–131.

[14]Armstrong, B. H., "Spectrum Line Profiles: The Voigt Function," *Journal of Quantum Spectroscopy and Radiative Transfer,* Vol. 7, 1967, pp. 61–88.

[15]Fletcher, D. G., "Spatially-Resolved, Nonintrusive Measurements in a Nonreacting Scramjet Combustor Using Laser-Induced Iodine Fluorescence," Ph.D. Dissertation, Dept. of Mechanical and Aerospace Engineering, Univ. of Virginia, Charlottesville, VA, Jan. 1989.

[16]Churassy, S., Grenet, G., Gaillard, M. L., and Bacis, R., "Hyperfine Structure in the B↔X Transition of the Iodine Molecule Near the Head of the 12-0 Band, By Laser Spectroscopy of a Pure Iodine Supersonic Jet," *Optics Communications,* Vol. 30, No. 1, July 1979, pp. 41–46.

[17]Hartfield, R. J., Jr., "Planar Measurement of Flow Field Parameters in Nonreacting Supersonic Flows with Laser-Induced Iodine Fluorescence," Ph.D. Dissertation, Dept. of Mechanical and Aerospace Engineering, Univ. of Virginia, Charlottesville, VA, May 1991.

[18]Westblom, U., and Alden, M., "Spatially Resolved Flow Velocity Measurements Using Laser-Induced Fluorescence from a Pulsed Laser," *Optics Letters,* Vol. 14, No. 1, 1989, pp. 9–11.

[19]Hollo, S. D., "Planar Mole Fraction and Velocity Imaging of Compressible Mixing in a Nonreacting Mach 2 Combustor," M.S. Thesis, Dept. of Mechanical and Aerospace Engineering, Univ. of Virginia, Charlottesville, VA, May 1991.

[20]Eklund, D. R., Northam, G. B., and Hartfield, R. J., Jr., "A Detailed Investigation of Staged Normal Injection into a Mach 2 Flow," CPIA Publication 557, Vol. 3, 27th JANNAF Combustion Meeting, F. E. Warren Air Force Base, Cheyenne, WY, Nov. 1990, pp. 115–129.

[21]McDaniel, J. C., Fletcher, D. G., Hartfield, R. J., Jr., and Hollo, S. D., "Staged Transverse Injection into Mach 2 Flow Behind a Rearward-Facing Step: A 3-D Compressible Test Case for Hypersonic Combustor Code Validation," Third International Aerospace Plane Conference, AIAA Paper 91-5071, Orlando, FL, Dec. 1991.

[22]Eklund, D. R., private communication, NASA Langley Research Center, Hampton, VA, Aug. 1990.